

The spectral density of dense random networks and the breakdown of the Wigner law

Fernando L. Metz*

*Physics Institute, Federal University of Rio Grande do Sul, 91501-970 Porto Alegre, Brazil and
London Mathematical Laboratory, 18 Margrave Gardens, London W6 8RH, United Kingdom*

Jeferson D. Silva

Physics Institute, Federal University of Rio Grande do Sul, 91501-970 Porto Alegre, Brazil

Although the spectra of random networks have been studied for a long time, the influence of network topology on the dense limit of network spectra remains poorly understood. By considering the configuration model of networks with four distinct degree distributions, we show that the spectral density of the adjacency matrices of dense random networks is determined by the strength of the degree fluctuations. In particular, the eigenvalue distribution of dense networks with an exponential degree distribution is governed by a simple equation, from which we uncover a logarithmic singularity in the spectral density. We also derive a relation between the fourth moment of the eigenvalue distribution and the variance of the degree distribution, which leads to a sufficient condition for the breakdown of the Wigner law for dense random networks. Based on the same relation, we propose a classification scheme of the distinct universal behaviours of the spectral density in the dense limit. Our theoretical findings should lead to novel insights on the mean-field behaviour of models defined on graphs.

I. INTRODUCTION

A random network or graph is a collection of nodes joined by edges following a probabilistic rule. Random networks are formidable tools to model large assemblies of interacting units, being them neurons in the brain, computers and routers in the Internet, or persons forming a friendship network [1]. Motivated by our increasing ability to collect and process vast amounts of empirical data, the theory of random networks has experienced an enormous progress, leading to important insights in physics, biology, and sociology [2]. The implications of the structure of networks to the dynamical processes occurring on them remains a fundamental topic in network theory [3].

Dynamical processes on networks are to a large extent governed by the spectrum of the adjacency matrix. This is a random matrix where each entry equals the strength of the interaction between a pair of nodes. The study of a broad range of problems amounts to linearize a large set of differential equations [4–6], coupled through a random network, around a stationary state, whose stability is ultimately determined by the eigenvalue distribution of the adjacency matrix. Examples in this context are the study of the epidemic threshold for the spreading of diseases [7], the synchronization transition in networks of coupled oscillators [8, 9], and the functional stability of large biological systems, such as gene regulatory networks [10, 11], ecosystems [12–14], and neural networks [15–17]. Therefore, the problem of how the network architecture influences the spectrum of the adjacency matrix has attracted considerable research efforts [4, 18–24].

Synthetic models of random networks provide a controlled way to study the role of the network structure on the spectrum of the adjacency matrix. The degree sequence is the most basic tool to characterize the graph structure [1]. The degree of a node counts the number of edges attached to the node, while

the degree sequence specifies all network degrees. When a network has an infinitely large number of constituents, it is natural to consider the degree distribution, i.e. the fraction of nodes with a certain degree, instead of dealing with the degree sequence. The configuration model stands out as one of the most fundamental and versatile models of random graphs [1, 25–27], since it enables the degree distribution to be freely specified, while keeping the pattern of interconnections entirely random. From a practical viewpoint, the configuration model resolves one of the main shortcomings of Erdős–Rényi random graphs [28–30], namely its Poisson degree distribution, which has little resemblance with the long-tailed degree distributions found in empirical networks [31, 32]. The priceless possibility to fix the degree distribution of a random graph is not only useful to model the structure of empirical networks, but it offers the ideal setting to examine the impact of degree fluctuations on the spectrum of the adjacency matrix.

There has been a significant amount of numeric and analytic work on the spectral properties of adjacency random matrices [4, 18–24, 33–40]. A remarkable analytic result is the set of exact and mathematically rigorous equations determining the eigenvalue distribution of the configuration model [35–37, 41]. These equations form a natural starting point to study the impact of degree fluctuations on network spectra. Unfortunately, aside from a few particular cases [23, 38, 41], these equations can be analytically solved only in the dense limit [35, 36], when the mean degree becomes infinitely large and random networks approach a fully-connected structure.

The analytic solution for the dense limit of the aforementioned equations is at the root of perturbative and non-perturbative approximations for the eigenvalue distribution of large-degree random networks [19, 33, 42]. With the exception of graphs with a power-law degree distribution [18, 20, 34], whose moments are divergent, one expects that the eigenvalue distribution of undirected random networks converges, in the dense limit, to the Wigner law of random matrix theory [43], reflecting a high level of universality. In fact, this expectation has been confirmed numerically [18] and analytically [35, 36], although these results usually apply to

* fmetzmetz@gmail.com

Erdős-Rényi random graphs. The general problem of how the structure of dense random networks influences their eigenvalue spectra, and the universal status of the Wigner law for undirected networks, have eluded a careful analysis. The purpose of our work is to fill this gap.

In this work we study the dense limit of the eigenvalue distribution of undirected networks drawn from the configuration model. We analyse four examples of degree distributions, in which all moments are finite and the variances scale differently with the average degree. Building on a set of exact equations [35, 36], we show that the dense limit of the eigenvalue distribution is determined by the degree fluctuations, in contrast to the expected results from random matrix theory. In particular, we derive an equation yielding the eigenvalue distribution of dense random graphs with an exponential degree distribution [27], from which we unveil the existence of a logarithmic divergence in the spectral density and the absence of sharp spectral edges, i.e., the eigenvalue distribution of exponential random graphs is supported on the entire real line. These are remarkable differences with respect to the Wigner law of random matrix theory [43]. Based on an exact calculation of the fourth moment of the eigenvalue distribution, we obtain a sufficient condition for the breakdown of the Wigner law. This condition is given only in terms of the variance of the degree distribution. We finish the paper by conjecturing a classification of the different universal behaviours of the eigenvalue distribution of the configuration model in the dense limit, based on an exponent characterizing how the variance of the degree distribution diverges for increasing mean degree.

Our paper is organized as follows. In the next section we define the adjacency matrix of networks and the spectral density. Section III introduces the configuration model and defines the degree distributions studied in this work. In section IV, we present numeric and analytic results for the dense limit of the spectral density for each example of degree distribution. The condition for the breakdown of the Wigner law and the classification of the different universal behaviours are discussed in section V. We summarize our results and conclude in section VI.

II. THE ADJACENCY MATRIX OF RANDOM NETWORKS

Let N be the total number of network nodes. The set of binary random variables $\{C_{ij}\}_{i,j=1,\dots,N}$ specifies the network structure: if $C_{ij} = 1$, there is an undirected link $i \leftrightarrow j$ between nodes i and j , while $C_{ij} = 0$ means this link is absent. We also associate a random weight $A_{ij} \in \mathbb{R}$ to each edge $i \leftrightarrow j$, which accounts for the interaction strength between nodes i and j . We consider undirected simple random networks that have no self-edges nor multi-edges, in which $C_{ij} = C_{ji}$, $A_{ij} = A_{ji}$, and $C_{ii} = 0$.

The degree $K_i = \sum_{j=1}^N C_{ij}$ of node i is a random variable that counts the number of nodes attached to i , while the degree sequence K_1, \dots, K_N provides global information on the fluctuations of the network connectivity. In the limit $N \rightarrow \infty$, it is more convenient to work with the degree

distribution

$$p_k = \lim_{N \rightarrow \infty} \frac{1}{N} \sum_{i=1}^N \delta_{k, K_i}, \quad (1)$$

where δ is the Kronecker symbol. The average degree c and the variance σ^2 of p_k read

$$c = \sum_{k=0}^{\infty} k p_k, \quad \sigma^2 = \sum_{k=0}^{\infty} p_k (k - c)^2.$$

The degree distribution p_k is one of the primary quantities to characterize the structure of random networks in the limit $N \rightarrow \infty$.

We will study the eigenvalue distribution of the $N \times N$ symmetric adjacency matrix \mathbf{S} , with elements defined as

$$S_{ij} = \frac{C_{ij} A_{ij}}{\sqrt{c}}. \quad (2)$$

The adjacency matrix fully encodes the network structure, along with the coupling strengths between adjacent nodes. The empirical spectral measure of the adjacency matrix is given by

$$\rho_N(\lambda) = \frac{1}{N} \sum_{\alpha=1}^N \delta(\lambda - \lambda_\alpha), \quad (3)$$

where $\lambda_1, \dots, \lambda_N$ are the (real) eigenvalues of \mathbf{S} . By introducing the $N \times N$ resolvent matrix

$$\mathbf{G}(z) = (z - \mathbf{S})^{-1}, \quad (4)$$

with $z = \lambda - i\eta$ on the lower half complex plane, the empirical spectral measure follows from the diagonal elements of $\mathbf{G}(z)$

$$\rho_N(\lambda) = \frac{1}{\pi N} \lim_{\eta \rightarrow 0^+} \sum_{i=1}^N \text{Im} G_{ii}(z). \quad (5)$$

In the limit $N \rightarrow \infty$, the empirical mean of $\text{Im} G_{ii}(z)$ normally converges to its ensemble averaged value, obtained from the distribution of \mathbf{S} , which implies that $\rho(\lambda) = \lim_{N \rightarrow \infty} \rho_N(\lambda)$ is well-defined. Here we will study the spectral density $\rho(\lambda)$ when the average degree grows to infinity, hence the limit $c \rightarrow \infty$ is performed *after* $N \rightarrow \infty$. The scaling of the elements S_{ij} with the average degree c in Eq. (2) ensures the spectral density has a finite variance when $c \rightarrow \infty$.

III. THE CONFIGURATION MODEL OF NETWORKS

We study random networks with arbitrary degree distributions, known as the configuration model of networks [1, 25–27], where p_k is specified at the outset. A single instance of the adjacency matrix of the configuration model is created as follows. First, the degrees K_1, \dots, K_N are drawn independently from a common distribution p_k . After assigning K_i stubs of edges to each node i ($i = 1, \dots, N$), a pair

of stubs is uniformly chosen at random and then connected to form an edge. This last step is repeated on the remainder stubs until there are no stubs left, and the outcome is a particular matching of the stubs with the prescribed random degrees K_1, \dots, K_N . We do not allow for the existence of self-edges and multi-edges in the random network. We set $S_{ij} = A_{ij}/\sqrt{c}$ if there is an edge connecting nodes i and j , and $S_{ij} = 0$ otherwise. The coupling strengths $\{A_{ij}\}_{i,j=1,\dots,N}$ are i.i.d. random variables drawn from a common distribution $P_A(a)$. We refer to [1] for other properties and subtleties of the configuration model. In the limit $N \rightarrow \infty$, the ensemble of adjacency random matrices \mathbf{S} constructed from this procedure is specified by the degree distribution p_k and the distribution of weights $P_A(a)$. This is probably the simplest network model that allows to clearly exploit the influence of degree fluctuations on the spectral properties of \mathbf{S} .

We will present results for regular, Poisson, exponential, and Borel degree distributions. The analytic expression for p_k in each case, together with the variance σ^2 , is displayed in table I. These degree distributions obey the following properties: (i) p_k is parametrized solely in terms of the mean degree c ; (ii) all moments of p_k are finite for $c < \infty$; (iii) for sufficiently large c , the variances obey $\sigma_{\text{reg}}^2 < \sigma_{\text{pois}}^2 < \sigma_{\text{exp}}^2 < \sigma_{\text{bor}}^2$. These four examples of degree distributions are very convenient to study, in a controllable way, the effect of degree fluctuations on random networks as we increase c . Indeed, we can compare for $c \gg 1$ the spectral density of networks with the same average degree, but with increasing variances σ^2 . We do not consider here random networks with power-law degree distributions [31, 32], since in this case higher-order moments of p_k diverge already for finite c .

	Regular	Poisson	Exponential	Borel
p_k	$\delta_{k,c}$	$\frac{e^{-c} c^k}{k!}$	$\frac{1}{c+1} \left(\frac{c}{c+1}\right)^k$	$\frac{e^{-\frac{(c-1)}{c}k}}{k!} \left[\frac{k(c-1)}{c}\right]^{k-1}$
σ^2	0	c	$c^2 + c$	$c^3 - c^2$

TABLE I. The analytic expression for the degree distribution p_k and the corresponding variance σ^2 in the case of regular, Poisson, exponential, and Borel random networks. The Borel degree distribution is supported in $k \geq 1$, the degree distribution of regular graphs is supported at $k = c$, and both Poisson and exponential degree distributions are supported in $k \geq 0$.

Although the Borel degree distribution is not commonly employed in the study of random networks, it exhibits an exponential tail that decays slower than the tail of the exponential degree distribution, which makes the Borel distribution well-suited to our analysis. The Borel distribution, introduced in the context of queuing theory [44, 45], also appears as the distribution of the total progeny in a Galton-Watson branching process with Poisson distributed degrees [46]. Figure 1 illustrates the Borel degree distribution for different average degrees. Note that p_k in figure 1 is highly skewed, its mode is located at $k = 1$, and the tail of p_k decays as $\ln p_k \sim \left(\frac{1}{c} + \ln\left(\frac{c-1}{c}\right)\right)k$ for $k \gg 1$. We point out that all network models considered here have exponentially decaying

degree distributions.

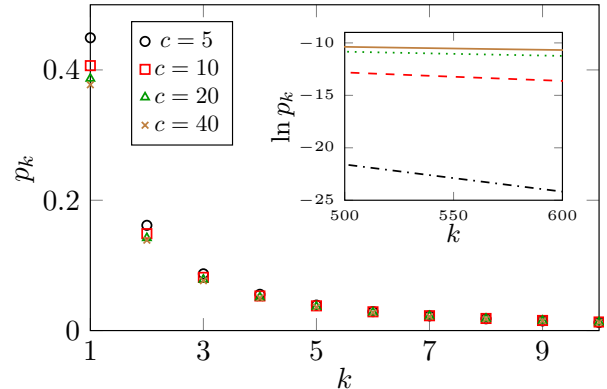


FIG. 1. The Borel degree distribution p_k (see table I) for different values of the average degree c . The inset depicts the exponential tail of p_k for large k . The values of c in the inset are $c = 40$ (solid line), $c = 20$ (dotted line), $c = 10$ (dashed line), and $c = 5$ (dot-dashed line).

IV. THE DENSE LIMIT OF THE SPECTRAL DENSITY

The configuration model of networks has a key property: in the limit $N \rightarrow \infty$, the set of nodes in the neighborhood of a given node, drawn uniformly from the network, is arranged in a tree-like structure [41]. Nevertheless, the topology of random networks is fundamentally different from a Cayley tree [47], in the sense that boundary nodes are absent in the limit $N \rightarrow \infty$, but their average length scales as $\ln N$ for $N \gg 1$. Roughly speaking, a random network can be seen as a Cayley tree with fluctuating degrees, wrapped onto itself.

In the limit $N \rightarrow \infty$, the spectral density is obtained from

$$\rho(\lambda) = \frac{1}{\pi} \lim_{\eta \rightarrow 0^+} \int_{\text{Im}g \geq 0} d^2g \mathcal{P}(g) \text{Im}g, \quad (6)$$

where $d^2g \equiv d\text{Re}g d\text{Im}g$, and $\mathcal{P}(g)$ is the joint distribution of the real and imaginary parts of $G_{ii}(z)$. The symbol $\int_{\text{Im}g \geq 0}$ represents an integral over $g \in \mathbb{C}$ restricted to the upper half complex plane. The distribution of the resolvent follows from the solution of the coupled equations [35, 36]

$$\mathcal{P}(g) = \sum_{k=0}^{\infty} p_k \int_{\text{Im}g \geq 0} \left[\prod_{\ell=1}^k d^2g_{\ell} \mathcal{P}_{\text{cav}}(g_{\ell}) \right] \times \left\langle \delta \left[g - \left(\frac{1}{z - \frac{1}{c} \sum_{\ell=1}^k A_{\ell}^2 g_{\ell}} \right) \right] \right\rangle_{A_1, \dots, A_k}, \quad (7)$$

$$\mathcal{P}_{\text{cav}}(g) = \sum_{k=0}^{\infty} \frac{k p_k}{c} \int_{\text{Im}g \geq 0} \left[\prod_{\ell=1}^{k-1} d^2g_{\ell} \mathcal{P}_{\text{cav}}(g_{\ell}) \right] \times \left\langle \delta \left[g - \left(\frac{1}{z - \frac{1}{c} \sum_{\ell=1}^{k-1} A_{\ell}^2 g_{\ell}} \right) \right] \right\rangle_{A_1, \dots, A_{k-1}} \quad (8)$$

where $\langle \dots \rangle_{A_1, \dots, A_L}$ denotes the average over the independent interaction strengths A_1, \dots, A_L , distributed according to $P_A(a)$. The quantity $\mathcal{P}_{\text{cav}}(g)$ is the joint distribution of the real and imaginary parts of the resolvent elements $G_{ii}^{(j)}(z)$ on the cavity graph [35, 48], defined as the graph where an arbitrary node j and all its edges have been removed. Equations (7) and (8) have been derived using both the cavity [35, 48] and the replica method [36] of disordered systems, based on the locally tree-like structure of the configuration model. Equations (6-8) are exact in the limit $N \rightarrow \infty$, constituting the point of departure to study the dense limit $c \rightarrow \infty$ of the spectral density $\rho(\lambda)$.

Let $F(G)$ be an arbitrary function of the complex random variable G distributed as $\mathcal{P}_{\text{cav}}(g)$. By defining the average of $F(G)$

$$\langle F(G) \rangle = \int_{\text{Im}g \geq 0} d^2g \mathcal{P}_{\text{cav}}(g) F(g),$$

we can use Eq. (8) and rewrite the above expression as

$$\langle F(G) \rangle = \int_{\text{Im}q \geq 0} d^2q \mathcal{W}_{\text{cav}}(q) F\left(\frac{1}{z-q}\right), \quad (9)$$

where we introduced the distribution of $Q' \equiv \frac{1}{c} \sum_{\ell=1}^{K-1} A_\ell^2 G_\ell$

$$\mathcal{W}_{\text{cav}}(q) = \sum_{k=0}^{\infty} \frac{k p_k}{c} \int_{\text{Im}g \geq 0} \left[\prod_{\ell=1}^{k-1} d^2g_\ell \mathcal{P}_{\text{cav}}(g_\ell) \right] \times \left\langle \delta \left(q - \frac{1}{c} \sum_{\ell=1}^{k-1} A_\ell^2 g_\ell \right) \right\rangle_{A_1, \dots, A_{k-1}}. \quad (10)$$

Following an analogous procedure, we can also rewrite the spectral density in terms of the distribution $\mathcal{W}(q)$ of the random variable $Q \equiv \frac{1}{c} \sum_{\ell=1}^K A_\ell^2 G_\ell$

$$\rho(\lambda) = \frac{1}{\pi} \lim_{\eta \rightarrow 0^+} \int_{\text{Im}q \geq 0} d^2q \mathcal{W}(q) \text{Im} \left(\frac{1}{z-q} \right), \quad (11)$$

defined as

$$\mathcal{W}(q) = \sum_{k=0}^{\infty} p_k \int_{\text{Im}g \geq 0} \left[\prod_{\ell=1}^k d^2g_\ell \mathcal{P}_{\text{cav}}(g_\ell) \right] \times \left\langle \delta \left(q - \frac{1}{c} \sum_{\ell=1}^k A_\ell^2 g_\ell \right) \right\rangle_{A_1, \dots, A_k}. \quad (12)$$

We note that $\mathcal{W}(q)$ and $\mathcal{W}_{\text{cav}}(q)$ are distributions of sums of independent complex random variables containing a random number of terms. Thus, instead of working with the distributions of the resolvent, it is more convenient to extract the $c \rightarrow \infty$ limit of $\mathcal{W}(q)$ and $\mathcal{W}_{\text{cav}}(q)$. Let us introduce the characteristic functions $\varphi(p, t)$ and $\varphi_{\text{cav}}(p, t)$ of, respectively, $\mathcal{W}(g)$ and $\mathcal{W}_{\text{cav}}(g)$

$$\varphi(p, t) = \sum_{k=0}^{\infty} p_k \exp[kS(p, t)], \quad (13)$$

$$\varphi_{\text{cav}}(p, t) = \sum_{k=0}^{\infty} \frac{k p_k}{c} \exp[(k-1)S(p, t)], \quad (14)$$

with

$$S(p, t) = \ln \left[\int_{\text{Im}g \geq 0} d^2g \mathcal{P}_{\text{cav}}(g) \int_{-\infty}^{\infty} da P_A(a) \times \exp \left(-\frac{ipa^2 \text{Re}g}{c} - \frac{ita^2 \text{Im}g}{c} \right) \right]. \quad (15)$$

In order to study the dense limit $c \rightarrow \infty$, we expand $S(p, t)$ in powers of $1/c$, keeping in mind that the moments of $\mathcal{P}_{\text{cav}}(g)$ depend on c . The leading term

$$S_\infty(p, t) = -\frac{i \langle A^2 \rangle_A}{c} (p \text{Re} \langle G \rangle_\infty + t \text{Im} \langle G \rangle_\infty) \quad (16)$$

should yield dense limit $c \rightarrow \infty$ of the spectral density. Note that we assumed $\langle G \rangle$ converges to a well-defined limit $\langle G \rangle_\infty$ when $c \rightarrow \infty$. In order to proceed further, we specify the degree distribution p_k in Eqs. (13) and (14).

A. Regular and Poisson random graphs

Although it is well-known that the dense limit of $\rho(\lambda)$ converges to the Wigner law for regular and Poisson random graphs, it is instructive to illustrate our approach for these simple models, characterized by highly peaked degree distributions around the mean value c . Substituting the explicit forms of p_k (see table I) in Eqs. (13) and (14), and using the asymptotic behaviour of Eq. (16), we obtain

$$\varphi(p, t) = \varphi_{\text{cav}}(p, t) = e^{-i \langle A^2 \rangle_A (p \text{Re} \langle G \rangle_\infty + t \text{Im} \langle G \rangle_\infty)}, \quad (17)$$

which promptly leads to the Dirac delta distribution in the complex plane

$$\mathcal{W}(q) = \mathcal{W}_{\text{cav}}(q) = \delta(q - \langle A^2 \rangle_A \langle G \rangle_\infty). \quad (18)$$

The fact that the resolvent statistics of regular and Poisson random graphs are both described by the same characteristic function, Eq. (17), already demonstrates that these models exhibit the same universal behaviour for $c \rightarrow \infty$. The analytic expression for $\mathcal{W}_{\text{cav}}(q)$ allows to determine $\langle G \rangle_\infty$ through Eq. (9), which fulfils

$$\langle G \rangle_\infty = \frac{1}{z - \langle A^2 \rangle_A \langle G \rangle_\infty}, \quad (19)$$

while the spectral density simply follows from Eq. (11)

$$\rho(\lambda) = \frac{1}{\pi} \lim_{\eta \rightarrow 0^+} \text{Im} \left(\frac{1}{z - \langle A^2 \rangle_A \langle G \rangle_\infty} \right).$$

By solving the quadratic equation (19), we recover the Wigner law for the Gaussian ensembles of random matrix theory [43]

$$\rho(\lambda) = \begin{cases} \frac{1}{2\pi \langle A^2 \rangle_A} \sqrt{4 \langle A^2 \rangle_A - \lambda^2}, & \text{if } |\lambda| < 2\sqrt{\langle A^2 \rangle_A} \\ 0, & \text{if } |\lambda| \geq 2\sqrt{\langle A^2 \rangle_A}. \end{cases} \quad (20)$$

Figure 2 compares Eq. (20) with numerical results obtained from diagonalizing large adjacency matrices \mathcal{S} with average degree $c = 100$. The correspondence between the numerical data and the theoretical expression is excellent for both regular and Poisson random graphs.

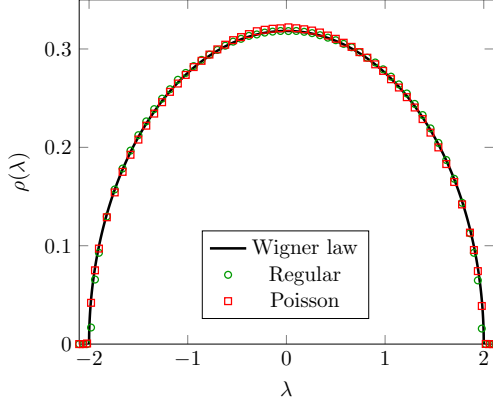


FIG. 2. The dense limit $c \rightarrow \infty$ of the spectral density of regular and Poisson random networks with coupling strengths drawn from $P_A(a) = \delta(a - 1)$. The solid line represents the Wigner law, Eq. (20), and the symbols are numerical diagonalization results obtained from 100 samples of $10^4 \times 10^4$ adjacency random matrices with $c = 100$.

B. Exponential random graphs

In this subsection we consider the dense limit of exponential random graphs, for which p_k decays slower than Poisson graphs for $k \gg 1$ (see table I). Exponential degree distributions have been observed in some examples of empirical networks, such as the North American power grid [49] and the neural network of the worm *C. Elegans* [50].

Inserting the expressions for $S_\infty(p, t)$ and p_k in Eqs. (13-14) and taking the limit $c \rightarrow \infty$, we obtain the asymptotic forms

$$\begin{aligned} \varphi(p, t) &= \frac{1}{1 + ip\langle A^2 \rangle_A \text{Re}\langle G \rangle_\infty + it\langle A^2 \rangle_A \text{Im}\langle G \rangle_\infty}, \\ \varphi_{\text{cav}}(p, t) &= \frac{1}{[1 + ip\langle A^2 \rangle_A \text{Re}\langle G \rangle_\infty + it\langle A^2 \rangle_A \text{Im}\langle G \rangle_\infty]^2}, \end{aligned}$$

which already show that the dense limit of $\rho(\lambda)$ is not described by the Wigner law in this case. The distributions $\mathcal{W}(q)$ and $\mathcal{W}_{\text{cav}}(q)$ are the Fourier transforms of their characteristic functions. Defining

$$\begin{aligned} \mathcal{K}(q, \epsilon) &= \int_{-\infty}^{\infty} \frac{dp dt}{4\pi^2} \exp(ip \text{Re}q + it \text{Im}q) \\ &\times [\epsilon + ip\langle A^2 \rangle_A \text{Re}\langle G \rangle_\infty + it\langle A^2 \rangle_A \text{Im}\langle G \rangle_\infty]^{-1}, \end{aligned} \quad (21)$$

with $\epsilon \geq 1$ an auxiliary parameter, $\mathcal{W}(q)$ and $\mathcal{W}_{\text{cav}}(q)$ are

obtained from

$$\mathcal{W}(q) = \mathcal{K}(q, \epsilon = 1), \quad \mathcal{W}_{\text{cav}}(q) = -\left. \frac{\partial \mathcal{K}(q, \epsilon)}{\partial \epsilon} \right|_{\epsilon=1}. \quad (22)$$

The solution of the integral in Eq. (21) is given by

$$\begin{aligned} \mathcal{K}(q, \epsilon) &= \frac{\Theta(\text{Im}q)}{\langle A^2 \rangle_A \text{Im}\langle G \rangle_\infty} \delta\left(\text{Re}q - \text{Im}q \frac{\text{Re}\langle G \rangle_\infty}{\text{Im}\langle G \rangle_\infty}\right) \\ &\times \exp\left(-\frac{\epsilon \text{Im}q}{\langle A^2 \rangle_A \text{Im}\langle G \rangle_\infty}\right), \end{aligned}$$

leading to the analytic expressions

$$\begin{aligned} \mathcal{W}(q) &= \frac{\Theta(\text{Im}q)}{\langle A^2 \rangle_A \text{Im}\langle G \rangle_\infty} \delta\left(\text{Re}q - \text{Im}q \frac{\text{Re}\langle G \rangle_\infty}{\text{Im}\langle G \rangle_\infty}\right) \\ &\times \exp\left(-\frac{\text{Im}q}{\langle A^2 \rangle_A \text{Im}\langle G \rangle_\infty}\right), \end{aligned} \quad (23)$$

$$\begin{aligned} \mathcal{W}_{\text{cav}}(q) &= \frac{\Theta(\text{Im}q) \text{Im}q}{[\langle A^2 \rangle_A \text{Im}\langle G \rangle_\infty]^2} \delta\left(\text{Re}q - \text{Im}q \frac{\text{Re}\langle G \rangle_\infty}{\text{Im}\langle G \rangle_\infty}\right) \\ &\times \exp\left(-\frac{\text{Im}q}{\langle A^2 \rangle_A \text{Im}\langle G \rangle_\infty}\right), \end{aligned} \quad (24)$$

where $\Theta(\dots)$ is the Heaviside step function.

As in the previous subsection, Eqs. (23) and (24) depend on $\langle G \rangle_\infty$, but this quantity can be determined through Eq. (9). Substituting $\mathcal{W}_{\text{cav}}(q)$ in (9) and calculating the integral, we get

$$\begin{aligned} \langle G \rangle_\infty &= \frac{z}{\langle A^2 \rangle_A^2 \langle G \rangle_\infty^2} \exp\left(-\frac{z}{\langle A^2 \rangle_A \langle G \rangle_\infty}\right) \\ &\times \text{Ei}\left(\frac{z}{\langle A^2 \rangle_A \langle G \rangle_\infty}\right) - \frac{1}{\langle A^2 \rangle_A \langle G \rangle_\infty}, \end{aligned} \quad (25)$$

with $\text{Ei}(\dots)$ denoting the complex exponential integral function. The solutions of the above equation yield the dense limit of the averaged resolvent $\langle G \rangle_\infty$ on the cavity graph [35, 48]. The expression for $\rho(\lambda)$ in terms of $\langle G \rangle_\infty$ follows in an analogous way, i.e., one inserts Eq. (23) in Eq. (11) and calculates the remainder integral

$$\begin{aligned} \rho(\lambda) &= \frac{1}{\pi} \lim_{\eta \rightarrow 0^+} \text{Im} \left[\frac{1}{\langle A^2 \rangle_A \langle G \rangle_\infty} \exp\left(-\frac{z}{\langle A^2 \rangle_A \langle G \rangle_\infty}\right) \right. \\ &\left. \times \text{Ei}\left(\frac{z}{\langle A^2 \rangle_A \langle G \rangle_\infty}\right) \right]. \end{aligned} \quad (26)$$

It is suitable to introduce the adimensional variable $\gamma(z) \equiv \frac{z}{\langle A^2 \rangle_A \langle G \rangle_\infty}$, in terms of which the spectral density is given by

$$\rho(\lambda) = \frac{1}{\pi} \text{Im} \left(\frac{z^2 + \gamma^2 \langle A^2 \rangle_A}{z \gamma^2 \langle A^2 \rangle_A} \right), \quad (27)$$

where $\gamma(z)$ solves the following equation

$$\langle A^2 \rangle_A \gamma = \frac{z^2}{\gamma^2 e^{-\gamma} \text{Ei}(\gamma) - \gamma}. \quad (28)$$

Equations (27) and (28) constitute one of the main results of this paper. In contrast to the resolvent Eq. (19), whose analytic solution yields the Wigner law, the fixed-point Eq. (28) for the $c \rightarrow \infty$ limit of exponential graphs has no analytic solution for arbitrary z . The spectral density obtained from the numerical solutions of Eq. (28) is shown in figure 3-(a), together with direct diagonalization of large adjacency matrices of exponential random graphs with $c = 100$. The agreement between these two different approaches is excellent, confirming the exactness of Eqs. (27) and (28).

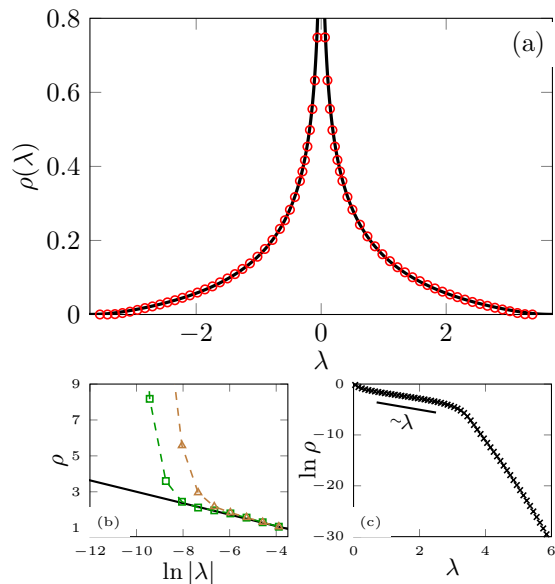


FIG. 3. Dense limit of the spectral density $\rho(\lambda)$ of random networks with an exponential degree distribution and coupling strengths drawn from $P_A(a) = \delta(a - 1)$. (a) Comparison between the theoretical results (black solid lines), obtained from the numerical solutions of Eqs. (27) and (28) for $\eta = 0$, and numerical diagonalizations (red circles) of 100 samples of $10^4 \times 10^4$ adjacency matrices with $c = 100$. (b) The logarithmic divergence of the spectral density for $|\lambda| \rightarrow 0$. The black solid line is the analytic result of Eq. (31), while the symbols are data derived from the numerical solutions of Eqs. (7) and (8) for $c = 80$ and two values of η : $\eta = 10^{-4}$ (brown triangles) and $\eta = 10^{-5}$ (green squares). (c) The exponential behaviour of the spectral density for large $|\lambda|$, obtained from the numerical solutions of Eqs. (27) and (28) for $\eta = 0$

Figure 3-(a) suggests that $\rho(\lambda)$ diverges at $\lambda = 0$. To study the singular behaviour of $\rho(\lambda)$ as $|\lambda| \rightarrow 0$, one needs to understand how $\gamma(z)$ vanishes as $|z| \rightarrow 0$. With a modest amount of foresight, we make the following *ansatz*

$$\gamma(z) = \beta_1 \frac{z}{\sqrt{\langle A^2 \rangle_A}} + \beta_2(z) \frac{z^2}{\langle A^2 \rangle_A}, \quad |z| \rightarrow 0, \quad (29)$$

where the function $\beta_2(z)$ is such that $\lim_{|z| \rightarrow 0} z^2 \beta_2(z) = 0$, and the coefficient β_1 is independent of z . Plugging this assumption for $\gamma(z)$ in the right hand side of Eq. (28) and expanding the result in powers of z up to $O(z^2)$, we find that the

above *ansatz* is consistent with Eq. (28) if β_1 and $\beta_2(z)$ are

$$\beta_1 = \pm i, \quad \beta_2(z) = -\frac{1}{2} \left[E + \ln \left(-\frac{\beta_1 z}{\sqrt{\langle A^2 \rangle_A}} \right) \right], \quad (30)$$

with E representing the Euler-Mascheroni constant. The last step is to substitute Eq. (29) in Eq. (27) and take the limit $\eta \rightarrow 0^+$, which leads to the logarithmic divergence

$$\rho(\lambda) = -\frac{1}{\pi \sqrt{\langle A^2 \rangle_A}} \left[E + \ln \left(\frac{|\lambda|}{\sqrt{\langle A^2 \rangle_A}} \right) \right], \quad (31)$$

for $|\lambda| \rightarrow 0$. The choice of the negative sign $\beta_1 = -i$ ensures that $\rho(\lambda)$ is non-negative. Figure 3-(b) compares Eq. (31) with the numerical solutions of the distributional Eqs. (7) and (8) for $c = 80$ using a Monte-Carlo method, also known as the population dynamics algorithm [35, 36, 48]. The numerical results lie on the top of the theoretical curve up to a certain $|\lambda_*|$, below which the numerical data for $\rho(\lambda)$ deviates from the logarithmic behaviour of Eq. (31). As η decreases, $|\lambda_*|$ shifts towards smaller values, confirming that the discrepancy between the numerical data and Eq. (31) is an artifact due to the finite values of η employed in the numerical solutions of Eqs. (7) and (8).

As a final important property, we inspect the behaviour of $\rho(\lambda)$ for $|\lambda| \gg 1$. As illustrated in figure 3-(c), $\rho(\lambda)$ displays a crossover from an exponential behaviour $\ln \rho(\lambda) \propto -\lambda$ to a faster decay for increasing $|\lambda|$, indicating that the spectral density does not have sharp spectral edges, but instead it is supported on the entire real line. This is also consistent with a stability analysis of the fixed-point Eq. (28), which shows that the complex solution for $\gamma(z)$ remains stable for $|\lambda| \gg 1$. We point out that a perturbative study of Eq. (28) for $|\lambda| \gg 1$ is not able to capture the analytic form describing the tails of $\rho(\lambda)$. This should not come as a surprise, as the tails of $\rho(\lambda)$ are normally caused by rare statistical fluctuations in the graph structure [33, 42].

C. Borel random graphs

As a final example of network model, we present results for random networks with a Borel degree distribution (see table I). In this case, our approach to derive analytic expressions for $\varphi(p, t)$ and $\varphi_{\text{cav}}(p, t)$ is not useful, because the probability generating function of the Borel degree distribution does not have a closed analytic form [46]. Thus, we obtain results through the numerical solution of Eqs. (7) and (8) using the population dynamics algorithm [35, 36, 48]. For Borel random graphs, the ratio σ/\sqrt{c} diverges as $c \rightarrow \infty$, which is precisely what renders this model interesting in comparison to Poisson and exponential graphs.

Figure 4 illustrates the evolution of the spectral density for increasing average degree. Similarly to exponential random graphs, the spectral density is not described by the Wigner law of random matrix theory, although the values of c in figure 4 are not large enough to observe the dense limit of $\rho(\lambda)$. We do not present results for larger values of c than those in

figure 4 because the population dynamics algorithm becomes prohibitively time consuming for increasing c , due to the large variance of the Borel degree distribution.

Among the distinctive features of $\rho(\lambda)$, we note the existence of δ -peaks for all values of c . These peaks are often located at the eigenvalues of finitely connected graph components [22, 36, 40, 51] and they usually disappear for large c , as the fraction of nodes belonging to the giant connected component converges to one in the dense limit [1]. Here, instead, we note these δ -peaks survive for $c \gg 1$. This occurs because the mode of the Borel degree distribution is located at $k = 1$, independently of c , and p_1 converges to a finite value $1/e$ in the limit $c \rightarrow \infty$. Hence we expect that, even for $c \rightarrow \infty$, a significant fraction of nodes will belong to open chains of finite length. Indeed, the eigenvalues of the adjacency matrices of paths or open chains containing one and two edges, with coupling strengths $1/\sqrt{c}$, are $\{-1/\sqrt{c}, 1/\sqrt{c}\}$ and $\{0, -\sqrt{2}/\sqrt{c}, \sqrt{2}/\sqrt{c}\}$, respectively. These eigenvalues correspond precisely with the positions of the δ -peaks in figure 4.

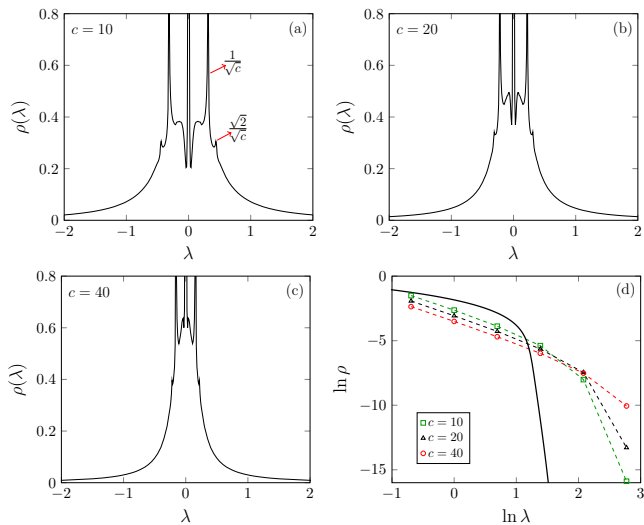


FIG. 4. The spectral density of random networks from the configuration model with a Borel degree distribution (see table I) for different average degrees c and coupling strengths drawn from $P_A(a) = \delta(a-1)$. All results are obtained from the numerical solutions of Eqs. (7) and (8) using the population dynamics algorithm with $\eta = 10^{-3}$ (subfigures (a), (b), and (c)) and $\eta = 10^{-4}$ (subfigure (d)). Subfigures (a), (b), and (c) show the spectral density of Borel random graphs for different c . Figure (a) also indicates the positive eigenvalues of open chains with one and two edges, and their correspondence with the position of δ -peaks. Figure (d) exhibits results for the tails of $\rho(\lambda)$. The symbols are results for Borel degree distributions with different c , while the solid black curve shows the tail of $\rho(\lambda)$ for exponential dense random graphs as a comparison (see also figure 3). The dashed lines are just a guide to the eye.

We have also inspected the tails of the spectral density of Borel random graphs. According to figure 4-(d), the behaviour of $\rho(\lambda)$ as a function of λ is consistent with a power-law decay up to a certain threshold λ_p , above which the data

clearly deviates from a straight line. As a matter of fact, we have confirmed that $\rho(\lambda)$ decreases as $\eta \rightarrow 0^+$ for values of λ larger than those appearing in figure 4-(d). In spite of that, the overall tendency of the data for increasing c suggests that $\rho(\lambda)$ does decay as a power-law in the limit $c \rightarrow \infty$. The results in figure 4 are insufficient to extract the exponent characterizing the power-law tails of $\rho(\lambda)$ for $c \rightarrow \infty$, since the spectral density has not reached its limiting behaviour for $c = 40$. Taken together, these results indicate that $\rho(\lambda)$ is supported on the entire real line.

V. THE FOURTH MOMENT OF THE EIGENVALUE DISTRIBUTION

The results of the previous section show that the dense limit of $\rho(\lambda)$ depends on the degree distribution of the configuration model. The scope of the Wigner law is apparently limited to models where p_k becomes highly concentrated around the mean degree for $c \rightarrow \infty$. In this section we derive a simple equation that reveals the influence of degree fluctuations on the spectral density, giving an exact condition for the breakdown of the Wigner law. We end up this section by proposing a classification of the different universal behaviours of the dense limit of $\rho(\lambda)$ for the configuration model of networks.

It is natural to characterize the statistics of random variables by computing the ratio between their moments. In the case of locally tree-like random networks, the odd moments of $\rho(\lambda)$ are zero and the simplest adimensional parameter of this type is the kurtosis $K_N(c)$

$$K_N(c) = \frac{\int_{-\infty}^{\infty} d\lambda \lambda^4 \rho_N(\lambda)}{\left[\int_{-\infty}^{\infty} d\lambda \lambda^2 \rho_N(\lambda) \right]^2} = \frac{\text{Tr} \mathbf{S}^4}{(\text{Tr} \mathbf{S}^2)^2}, \quad (32)$$

where we used the definition of the empirical spectral measure, Eq. (3). When $A_{ij} = \sqrt{c} \forall i, j$, the trace $\text{Tr} \mathbf{S}^n$ ($n = 2, 3, \dots$) is the total number of closed walks of length n in the graph, where the length of a walk between nodes i and j is the number of edges that a walker traverses when going from one node to the other [52]. The relation between the moments of $\rho_N(\lambda)$ and $\text{Tr} \mathbf{S}^n$ is very important in spectral graph theory, as it connects the eigenvalue statistics with the network structural properties [52]. The limit $N \rightarrow \infty$ must be taken before the $c \rightarrow \infty$ limit.

The trace of the second power of the adjacency matrix \mathbf{S} reads

$$\text{Tr} \mathbf{S}^2 = \frac{1}{c} \sum_{i=1}^N \sum_{j \in \partial_i} A_{ij}^2, \quad (33)$$

where ∂_i represents the set of nodes connected to i . For $N \rightarrow \infty$, we obtain

$$\lim_{N \rightarrow \infty} \frac{1}{N} \text{Tr} \mathbf{S}^2 = \frac{1}{c} \left\langle \sum_{j \in \partial_i} A_{ij}^2 \right\rangle_{A,K} = \langle A^2 \rangle_A, \quad (34)$$

with $\langle \dots \rangle_{A,K}$ denoting the ensemble average over the degrees and the coupling strengths. The trace of the fourth power can

be written as

$$c^2 \text{Tr} \mathbf{S}^4 = 2 \sum_{i=1}^N \sum_{j,r \in \partial_i} A_{ij}^2 A_{ri}^2 - \sum_{i=1}^N \sum_{j \in \partial_i} A_{ij}^4 + \sum_{i=1}^N \sum_{j \in \partial_i} \sum_{k \in \partial_j \setminus i} \sum_{r \in \partial_k \setminus j} C_{ir} A_{ij} A_{jk} A_{kr} A_{ri}, \quad (35)$$

where $\partial_j \setminus i$ is the set of nodes adjacent to j , except for node $i \in \partial_j$. In the limit $N \rightarrow \infty$, the configuration model has a locally tree-like structure, cycles of length four are rare, and hence the last term on the right hand side of Eq. (35) gives only a subleading contribution, which can be neglected for $N \rightarrow \infty$, yielding the expression

$$\lim_{N \rightarrow \infty} \frac{1}{N} \text{Tr} \mathbf{S}^4 = \frac{2}{c^2} \langle K(K-1) \rangle_K \langle A^2 \rangle_A^2 + \frac{1}{c} \langle A^4 \rangle_A. \quad (36)$$

Thus, we obtain an exact analytic expression for the $N \rightarrow \infty$ limit of the kurtosis

$$K_\infty(c) = \frac{1}{c} \frac{\langle A^4 \rangle_A}{\langle A^2 \rangle_A^2} + \frac{2}{c} (c-1) + 2 \frac{\sigma^2}{c^2}, \quad (37)$$

valid for arbitrary degree distributions with first and second moments finite. Note that $K_\infty(c)$ is invariant under a rescaling of the adjacency matrix elements. Equation (37) shows how the kurtosis of the eigenvalue distribution is linked to the degree fluctuations.

Let us now establish some general conclusions about the dense limit of $\rho(\lambda)$. For $c \rightarrow \infty$, $K_\infty(c)$ behaves as

$$\lim_{c \rightarrow \infty} K_\infty(c) = K_w \left(1 + \lim_{c \rightarrow \infty} \frac{\sigma^2}{c^2} \right), \quad (38)$$

where $K_w = 2$ is the kurtosis of the Wigner distribution [43], Eq. (20). Equation (38) unveils the central role of the degree fluctuations to the $c \rightarrow \infty$ limit of $\rho(\lambda)$. It follows that

$$\lim_{c \rightarrow \infty} \frac{\sigma^2}{c^2} > 0 \quad (39)$$

is a *sufficient* condition for the breakdown of the Wigner law. One naturally expects that the eigenvalue statistics of network models that fulfil condition (39) is not described by the traditional results of random matrix theory.

Based on Eq. (38), we can also put forward a classification of the different universal behaviours of $\rho(\lambda)$ in the dense limit. Let us consider weighted undirected networks, defined by the adjacency matrix of Eq. (2), in which the variance of p_k scales as $\sigma^2 = Hc^\alpha$ for large c , with $H > 0$ and α arbitrary parameters. For this broad class of network models, the different universal behaviours of $\rho(\lambda)$ can be classified in terms of the exponent α that quantifies the strength of the degree fluctuations. For $\alpha < 2$, we have $\lim_{c \rightarrow \infty} K_\infty(c) = 2$, the degree distribution is highly peaked around the mean degree, and the dense limit of $\rho(\lambda)$ is given by the Wigner law. Regular and Poisson random graphs are the main examples of this class of random networks characterized by $\alpha < 2$.

For $\alpha > 2$, the limit $\lim_{c \rightarrow \infty} K_\infty(c)$ diverges and we expect $\rho(\lambda)$ decays as a power-law $\rho(\lambda) \sim |\lambda|^{-\beta}$ for $|\lambda| \gg 1$, with an exponent $3 < \beta < 5$. The lower bound on β is due to the finite variance of $\rho(\lambda)$ in the dense limit (see Eq. (34)). Borel random graphs are characterized by $\alpha > 2$. Finally, network models with $\alpha = 2$ have a finite kurtosis $\lim_{c \rightarrow \infty} K_\infty(c) = 2(1+H) > K_w$, whose precise value is determined by the prefactor H . Exponential random networks belong to this later class where $\alpha = 2$. The results presented in the previous section are entirely consistent with this classification scheme.

VI. FINAL REMARKS

Traditional random matrix theory deals with the spectral properties of large random matrices with independent and identically distributed elements, providing a theoretical framework to address the universal properties of large interacting systems [53]. It is widely known that the eigenvalue distribution of undirected random networks strongly deviates from the Wigner law of random matrix theory in the *sparse* regime [18, 19, 33, 35, 36, 40, 51], i.e., when the average degree c is finite. As c grows to infinity, random networks gradually become more fully-connected and one may expect that random matrix theory describes well the spectral properties of *dense* random networks. Here we show that this is generally not the case.

We have studied the spectral density of the adjacency matrix of networks drawn from the configuration model with four distinct degree distributions. Our main conclusion is that the dense limit of the spectral density is governed by the strength of the degree fluctuations. It turns out that the Wigner law of random matrix theory is recovered only when the degree distribution becomes, in the dense limit, highly concentrated around the mean degree. We have also derived an exact relation between the fourth moment of the eigenvalue distribution and the variance of the degree distribution, from which a sufficient condition for the breakdown of the Wigner law follows. We point out that the degree distributions considered in this work have exponentially decaying tails, implying that all moments of the degree distribution are finite (the moments diverge only in the dense limit).

From the results derived in this work, one expects that, in general, the circular law of random matrix theory [4, 37] should also fail in describing the spectral density of directed random networks in the dense limit. Following the techniques discussed in sections IV and V, the study of the eigenvalue distribution of directed networks in the dense limit is just around the corner.

Among the results in section IV, we highlight the analytic equation for the averaged resolvent (see Eq. (25)), which determines the spectral density of exponential random graphs in the dense limit. This equation has no analytic solution, in contrast to the analogous Eq. (19) yielding the Wigner law. We have derived important features of the spectral density of dense exponential graphs, such as the existence of a logarithmic singularity around the origin and the absence of sharp

spectral edges. In the case of dense random networks with a Borel degree distribution, we have studied the spectral density by solving numerically the exact Eqs. (7) and (8). The results in figure 4 indicate that the spectral density of dense Borel networks is also supported on the entire real line, exhibiting power-law tails for large eigenvalues and δ -peaks at the eigenvalues of finite-length open chains. Taken together, these results reveal remarkable differences with respect to the Wigner law.

Based on Eq. (38) for the fourth moment of the eigenvalue distribution, we have proposed a classification scheme of the different universal behaviours of the spectral density in the dense regime. The classification holds for network models in which the variance σ^2 of the degree distribution scales as $\sigma^2 \propto c^\alpha$ for $c \gg 1$. Networks with $\alpha < 2$ exhibit weak degree fluctuations and the spectral density converges to the Wigner law for $c \rightarrow \infty$. Networks with $\alpha > 2$ display strong degree fluctuations and the spectral density is characterized by a divergent fourth moment and power-law tails for $c \rightarrow \infty$. Finally, the spectral density of dense networks with $\alpha = 2$ has a finite fourth moment, whose value is larger than in the case of the Wigner distribution. In light of this, it would be interesting to design a network model with a degree distribution

that has finite moments and interpolates among the different classes.

Overall, our results shed light on the fundamental role of the degree fluctuations to the dense limit of random networks. The condition for the breakdown of the Wigner law, Eq. (39), should apply beyond the realm of network spectra, indicating whether the degree fluctuations are strong enough to cause the failure of classic mean-field models on dense networks, such as the Curie-Weiss model [47] and the Sherrington-Kirkpatrick model [54]. Thus, we expect our results will stimulate research towards a better understanding of the dense limit of various models defined on random graphs, including ferromagnetic and spin-glass models [55], social dynamics [56], neural networks [57], and synchronization [8].

ACKNOWLEDGEMENTS

FLM thanks London Mathematical Laboratory and CNPq/Brazil for financial support. JDS acknowledges a fellowship from the London Mathematical Laboratory.

-
- [1] M. Newman, *Networks: An Introduction* (OUP Oxford, 2010).
- [2] S. Bornholdt and H. Schuster, *Handbook of Graphs and Networks: From the Genome to the Internet* (Wiley, 2003).
- [3] A. Barrat, M. Barthélemy, and A. Vespignani, *Dynamical Processes on Complex Networks* (Cambridge University Press, 2008).
- [4] F. L. Metz, I. Neri, and T. Rogers, *Journal of Physics A: Mathematical and Theoretical* **52**, 434003 (2019).
- [5] I. Neri and F. L. Metz, “Spectral theory for the stability of dynamical systems on large oriented locally tree-like graphs,” (2019), [arXiv:1908.07092 \[cond-mat.stat-mech\]](https://arxiv.org/abs/1908.07092).
- [6] W. Tarnowski, I. Neri, and P. Vivo, *Phys. Rev. Research* **2**, 023333 (2020).
- [7] R. Pastor-Satorras, C. Castellano, P. Van Mieghem, and A. Vespignani, *Rev. Mod. Phys.* **87**, 925 (2015).
- [8] J. G. Restrepo, E. Ott, and B. R. Hunt, *Phys. Rev. E* **71**, 036151 (2005).
- [9] A. Arenas, A. Daz-Guilera, J. Kurths, Y. Moreno, and C. Zhou, *Physics Reports* **469**, 93 (2008).
- [10] Y. Chen, Y. Shen, P. Lin, D. Tong, Y. Zhao, S. Allesina, X. Shen, and C.-I. Wu, *National Science Review* **6**, 1176 (2019), <https://academic.oup.com/nsr/article-pdf/6/6/1176/32351125/nwz076.pdf>.
- [11] Y. Guo and A. Amir, “Stability of gene regulatory networks,” (2020), [arXiv:2006.00018 \[physics.bio-ph\]](https://arxiv.org/abs/2006.00018).
- [12] R. M. May, *Nature* **238**, 413414 (1972).
- [13] S. Allesina, J. Grilli, G. Barabás, S. Tang, and J. Aljadeff, *Nat. Commun.* **6**, 7842 (2015).
- [14] J. Grilli, T. Rogers, and S. Allesina, *Nat. Commun.* **7**, 12031 (2016).
- [15] H. Sompolinsky, A. Crisanti, and H. J. Sommers, *Phys. Rev. Lett.* **61**, 259 (1988).
- [16] K. Rajan and L. F. Abbott, *Phys. Rev. Lett.* **97**, 188104 (2006).
- [17] F. Schuessler, A. Dubreuil, F. Mastrogiuseppe, S. Ostojic, and O. Barak, *Phys. Rev. Research* **2**, 013111 (2020).
- [18] I. J. Farkas, I. Derényi, A.-L. Barabási, and T. Vicsek, *Phys. Rev. E* **64**, 026704 (2001).
- [19] S. N. Dorogovtsev, A. V. Goltsev, J. F. F. Mendes, and A. N. Samukhin, *Phys. Rev. E* **68**, 046109 (2003).
- [20] G. J. Rodgers, K. Austin, B. Kahng, and D. Kim, *Journal of Physics A: Mathematical and General* **38**, 9431 (2005).
- [21] T. Rogers, C. P. Vicente, K. Takeda, and I. P. Castillo, *Journal of Physics A: Mathematical and Theoretical* **43**, 195002 (2010).
- [22] R. Khn and J. van Mourik, *Journal of Physics A: Mathematical and Theoretical* **44**, 165205 (2011).
- [23] F. L. Metz, I. Neri, and D. Bollé, *Phys. Rev. E* **84**, 055101 (2011).
- [24] M. E. J. Newman, *Phys. Rev. E* **100**, 012314 (2019).
- [25] M. Molloy and B. Reed, *Random Structures & Algorithms* **6**, 161 (1995), <https://onlinelibrary.wiley.com/doi/pdf/10.1002/rsa.3240060204>.
- [26] M. MOLLOY and B. REED, *Combinatorics, Probability and Computing* **7**, 295305 (1998).
- [27] M. E. J. Newman, S. H. Strogatz, and D. J. Watts, *Phys. Rev. E* **64**, 026118 (2001).
- [28] R. Solomonoff and A. Rapoport, *The bulletin of mathematical biophysics* **13**, 107 (1951).
- [29] P. Erdős and A. Rényi, *Publicationes Mathematicae Debrecen* **6**, 290 (1959).
- [30] P. Erdős, *Publications of the Mathematical Institute of the Hungarian Academy of Sciences* **5**, 17 (1960).
- [31] R. Albert and A.-L. Barabási, *Rev. Mod. Phys.* **74**, 47 (2002).
- [32] A. Clauset, C. R. Shalizi, and M. E. J. Newman, *SIAM Review* **51**, 661 (2009), <https://doi.org/10.1137/070710111>.
- [33] G. J. Rodgers and A. J. Bray, *Phys. Rev. B* **37**, 3557 (1988).
- [34] K.-I. Goh, B. Kahng, and D. Kim, *Phys. Rev. E* **64**, 051903 (2001).

- [35] T. Rogers, I. P. Castillo, R. Kühn, and K. Takeda, *Phys. Rev. E* **78**, 031116 (2008).
- [36] R. Kühn, *Journal of Physics A: Mathematical and Theoretical* **41**, 295002 (2008).
- [37] T. Rogers and I. P. Castillo, *Phys. Rev. E* **79**, 012101 (2009).
- [38] I. Neri and F. L. Metz, *Phys. Rev. Lett.* **109**, 030602 (2012).
- [39] F. L. Metz and I. Pérez Castillo, *Phys. Rev. Lett.* **117**, 104101 (2016).
- [40] M. E. J. Newman, X. Zhang, and R. R. Nadakuditi, *Phys. Rev. E* **99**, 042309 (2019).
- [41] C. Bordenave and M. Lelarge, *Random Structures & Algorithms* **37**, 332 (2010), <https://onlinelibrary.wiley.com/doi/pdf/10.1002/rsa.20313>.
- [42] G. Semerjian and L. F. Cugliandolo, *Journal of Physics A: Mathematical and General* **35**, 4837 (2002).
- [43] G. Livan, M. Novaes, and P. Vivo, *Introduction to Random Matrices: Theory and Practice*, SpringerBriefs in Mathematical Physics (Springer International Publishing, 2018).
- [44] E. Borel, *C. R. Acad. Sci.* **214**, 452 (1942).
- [45] P. Consul, S. Kotz, and F. Famoye, *Lagrangian Probability Distributions* (Birkhäuser Boston, 2005).
- [46] H. Finner, P. Kern, and M. Scheer, *Insurance: Mathematics and Economics* **62**, 234 (2015).
- [47] R. Baxter, *Exactly Solved Models in Statistical Mechanics*, Dover books on physics (Dover Publications, 2007).
- [48] F. L. Metz, I. Neri, and D. Bollé, *Phys. Rev. E* **82**, 031135 (2010).
- [49] R. Albert, I. Albert, and G. L. Nakarado, *Phys. Rev. E* **69**, 025103 (2004).
- [50] L. A. N. Amaral, A. Scala, M. Barthélémy, and H. E. Stanley, *Proceedings of the National Academy of Sciences* **97**, 11149 (2000), <https://www.pnas.org/content/97/21/11149.full.pdf>.
- [51] M. Bauer and O. Golinelli, *Journal of Statistical Physics* **103**, 301 (2001).
- [52] P. van Mieghem, *Graph Spectra for Complex Networks* (Cambridge University Press, 2012).
- [53] G. Akemann, J. Baik, and P. Di Francesco, *The Oxford Handbook of Random Matrix Theory*, Oxford Handbooks in Mathematics Series (Oxford University Press, 2015).
- [54] D. Sherrington and S. Kirkpatrick, *Phys. Rev. Lett.* **35**, 1792 (1975).
- [55] M. Leone, A. Vázquez, A. Vespignani, and R. Zecchina, *Eur. Phys. Journal B* **28**, 191 (2002).
- [56] C. Castellano, S. Fortunato, and V. Loreto, *Rev. Mod. Phys.* **81**, 591 (2009).
- [57] A. Coolen, R. Kühn, and P. Sollich, *Theory of Neural Information Processing Systems* (Oxford University Press, 2005).